Infectious Diseases Diagnosis & Treatment
Guo X, et al. Infect Dis Diag Treat 6: 199.
www.doi.org/ 10.29011/2577- 1515.100199
www.gavinpublishers.com

OPEN ACCESS

GAVIN PUBLISHERS

Research Article

Inhibition of Human Coronaviruses by Piperidine-4-Carboxamides

Xin Guo[1], Ayan Kumar Ghosh[1], Halli Miller[1], Konstance Knox[2], Madhuchhanda Kundu[2], Francis Peterson[3], David J Meyers[4], Ravit Arav-Boger[1*]

[1]Department of Pediatrics, Division of Infectious Disease, Medical College of Wisconsin, Milwaukee, WI 53226, USA

[2]Coppe Healthcare Solutions, Waukesha, WI 53186, USA

[3]Department of Biochemistry, Medical College of Wisconsin, Milwaukee, WI 53226, USA

[4]Department of Pharmacology and Molecular Sciences, Johns Hopkins University School of Medicine, Baltimore, MD 21205, USA

***Corresponding author:** Ravit Arav-Boger, Department of Pediatrics, Division of Infectious Disease, Medical College of Wisconsin, Milwaukee, WI 53226, USA

Citation: Guo X, Ghosh AK, Miller H, Knox K, Kundu M, et al. (2022) Inhibition of Human Coronaviruses by Piperidine-4-Carboxamides. Infect Dis Diag Treat 6: 199. DOI: 10.29011/2577-1515.100199

Received Date: 4 September 2022; **Accepted Date:** 21 September 2022; **Published Date:** 26 September 2022

Abstract

Immunization efforts for the severe acute respiratory syndrome coronavirus 2 (SARS-CoV-2) have been successful in reducing disease severity. Yet new variants continue to emerge, as well as vaccine hesitancy from some, requiring ongoing efforts to identify antiviral agents for SARS-CoV-2 treatment. Here, we evaluated the *in vitro* activities of piperidine-4-carboxamide compound (NCGC2955) against human α- coronavirus NL63, β-coronaviruses OC43, and the alpha and delta variants of SARS-CoV-2 in several cell lines. NCGC2955 showed antiviral activity in NL63-infected Vero and MK2 cells: EC_{50} 2.5± 0.15 μM and 1.5 ± 0.2 μM, respectively. The cellular toxicity in both cell types was > 300 μM. The EC_{50} of NCGC2955 in OC43-infected human foreskin fibroblasts was 1.5 ± 0.01 μM, and a dose-response in reducing OC43 antigen was observed in Western blot analysis. NCGC2955 inhibited SARS-CoV-2 in both Vero E6 and Calu-3 cells. A comparison of the activity of NCGC2955 and a structurally related analog (153) in SARS-CoV-2-infected Calu-3 cells revealed similar EC_{50} (0.2 ± 0.02 μM and 0.11 ± 0.04 μM, respectively). Both compounds inhibited the delta variant in Calu-3 cells. This class of agents may be promising broad-spectrum antivirals that can be further developed for clinical use.

Keywords: Broad-spectrum antiviral; Coronaviruses; Piperidine-4-carboxamide; SARS-CoV-2.

Introduction

Coronavirus (CoV) disease 19 (COVID-19), the respiratory illness caused by Severe Acute Respiratory Syndrome CoV 2 (SARS-CoV-2) continues to spread and has severe global effects [1]. As waves of the pandemic continue, along with the emergence of highly transmissible variants, researchers are tasked with developing safe, cost-effective preventive and therapeutic measures, which have included highly effective vaccines [2,3]. Remdesivir (GS-5734), an inhibitor of the viral RNA-dependent RNA polymerase, was repurposed as one such therapeutic treatment for SARS-CoV-2. Although it showed promising results in clinical trials, there is continued debate around the drug's efficacy. Cases of infection despite immunization call for the development of antiviral therapeutics [4]. Molnapiravir and Paxlovid, two oral direct-acting antivirals were recently granted emergency use authorization based on clinical trials showing reduced risk of hospitalization or death [5,6].

The alpha- and beta-CoVs infect humans, and four CoVs are prevalent in the population: α-CoV - 229E and NL63, and β-CoV OC43 and HKU1 [7]. A high degree of maintaining essential functional domains has been shown with β-CoVs OC43, MERS-CoV, SARS-CoV, and SARS-CoV-2, yet their response to antiviral agents may be unique and also involve specific host cell response. The combination of lopinavir and ritonavir, for instance, showed benefits in patients infected with both SARS-CoV and MERS-CoV [8] but was not effective in adults infected with SARS-CoV-2 alone [9]. Several drugs studied until now for SARS-CoV-2 have been repurposed from other indications, to allow faster track therapeutics. Repurposed drugs fitting this definition include remdesivir, hydroxychloroquine (with or without azithromycin) and chloroquine, remdesivir, immune-modulating agents [10-12], and virus-neutralizing monoclonal antibodies [13].

Here we evaluated the anti-coronavirus activity of compound NCGC2955 and a structurally related analog (153), the latter a reported inhibitor of Western Equine Encephalitis virus [14,15]. NCGC2955 was reported by our group to inhibit human cytomegalovirus, a DNA virus which belongs to the family of herpesviruses [16]. Analysis of NCGC2955 revealed reproducible inhibition of α and β coronaviruses as well as SARS-CoV-2 at low μM concentrations. Compound 153, a structurally related analog of NCGC2955, also inhibited SARS-CoV-2 in Vero E6 and Calu-3 cells.

Materials and Methods

Cell lines, viruses, and compounds

Vero (Vervet monkey kidney epithelial cells, ATCC CCL-81, from Dr. Gary Hayward, Johns Hopkins University) and LLC-MK2 (Rhesus monkey kidney epithelial cells, ATCC CCL-7, from Dr. Kelly Henrickson, Medical College of Wisconsin) were cultured in DMEM (Millipore Sigma, St. Louis, MO) and supplemented with 10% FBS (Corning, Oneonta, NY, USA), penicillin and streptomycin, HEPES, L-glutamine, and amphotericin B. Human foreskin fibroblasts (ATCC, CRL-2088) were cultured in DMEM supplemented with 10% FBS. Calu-3 human lung adenocarcinoma cells (ATCC HTB-55) and Vero E6 monkey kidney cells (ATCC CRL-1586) were used for infection with SARS-CoV-2. HCoV-NL63 (Zeptometrix, Franklin, MA, USA) and HCoV-OC43 (ATCC VR-1558, from Dr. Kelly Henrickson) were used for infection of cells at a multiplicity of infection (MOI) of 0.001 unless otherwise specified. SARS-CoV-2 strain USA_WA1/2020 was used for infection of Vero E6 and Calu-3, at MOI of 0.05. SARS-CoV-2 strain GNL-1205 (from Dr. Kenneth Plante, University of Texas Medical Branch) was used for infection of Calu-3 cells, MOI-0.05.

Cells were cultured in DMEM supplemented with 4% FBS post-infection with NL63 and OC43 and either 2% or 4% FBS post-infection with SARS-CoV-2 along with varying concentrations of the compounds. Cells treated with DMSO were used as negative controls and emetine (Sigma-Aldrich, St. Louis, MO) or remdesivir (AoBioUS Gloucester, MA) were used as positive controls for CoV inhibition.

NCGC2955 *1-(4-(4-chlorobenzyl)-4H-thieno[3,2-b] pyrrole-5-carbonyl)-N-isopropylpiperidine-4-carboxamide* was purchased from Glixx Laboratories Inc (Hopkinton, MA Catalog No. GLXC-22518), and synthesized at the Synthetic Core Facility, Department of Pharmacology and Molecular Sciences, Johns Hopkins University School of Medicine as previously described [16]. The synthesis of analog 153 was also carried out at the Johns Hopkins School of Medicine Synthetic Core Facility as previously described [17]. The purity of all synthesized and purchased compounds used in bioassays was determined by HPLC using either a Phenomenex Luna C18 3.0 × 75 mm column with a 7 min gradient of 4-100% ACN in H_2O with 0.05% v/v TFA or a Higgins Analytical, Inc. Targa C18 5 μm 4.6 × 150 mm column with a 30 min gradient of 0-100% ACN in H_2O with 0.01% TFA and either absorbance detection at 254 nm or evaporative light scattering detection. All compounds used in bioassays exhibited NMR and MS data consistent with their structures and purities of >98% as determined by RP-HPLC.

Quantitative Real-Time Reverse-Transcription PCR (qRT-PCR) Analysis

Total cellular RNA was obtained from infected or non-infected cell cultures and isolated using the RNEasy Mini Kit (Qiagen, Germantown, MD), according to manufacturer's instructions. RNA was reverse transcribed to cDNA using RevertAid 1st Strand cDNA Synthesis Kit (Thermo Fisher Scientific, Waltham, MA), and quantified by real-time RT-PCR using PowerUP SYBR Green Master Mix (Thermo Fisher Scientific) following the manufacturer's instructions. Three sets of control wells were included in all qRT-PCR assays: no reverse transcriptase, no cDNA template, or water only. The following primer pairs were used: OC43-F: 5'-GCTCAGGAAGGTCTGCTCC-3', OC43-R: 5'-TCCTGCACTAGAGGCTCTGC-3' [18], NL63-F 5'-AGGACCTTAAATTCAGACAACGTTCT-3', NL63-R 5'-GATTACGTTTGCGATTACCAAGACT-3' [18], GAPDH-F 5'- TTGGTATCGTGGAAGGACTC -3', GAPDH-R 5'-ACAGTCTTCTGGGTGGCAGT -3' [19]. Real-time PCR was performed on a Bio-Rad CFX Connect system (Bio-Rad, Hercules, CA).

Quantitative RT-PCR

The CDC 2019-Novel Coronavirus (2019-nCOV) Real-Time RT-PCR Diagnostic Panel was used to measure inhibition of SARS-CoV-2 in Calu-3 and Vero E6 cells. The primer/

probe system is described below. To establish a standard curve, we used AccuPlex SARS CoV-2 Reference Material. The following primer sets were used: 2019-nCoV_N1-F5'-GACCCCAAAATCAGCGAAAT-3', 2019-nCoV_N1-R 5'-TCTGGTTACTGCCAGTTGAATCTG- 3', 2019-nCoV_N1 Probe: 5'-ACCCCGCATTACGTTTGGTGGACC- 3', 2019-nCoV. Relative viral RNA copies were calculated by 10^x where x represents log viral RNA copies/ml compared to infected cells.

Inhibition of SARS-CoV-2 in Vero E6 cells

An endpoint titration assay for $TCID/_{50}$ PFU determinations was used for SARS-CoV-2 inhibition in Vero E6. Vero E6 monolayers in 96 well plates were infected at MOI 0.05 with SARS CoV-2 in DMEM + 2% FBS and incubated for 1 hour at 37°C, 5% CO_2. Inoculum was aspirated, cells rinsed once with DMEM (100 µl) without FBS. Serial 2-fold dilutions of compounds in DMEM 2% FBS were added to duplicate wells and incubated for 72 hours at 37°C, 5% CO_2. Monolayers were stained with a 2% crystal violet in 20% methanol solution.

Toxicity assays

A 3-(4,5-dimethyl-2-thiazolyl)-2,5-diphenyl-2H-tetrazolium bromide (MTT) assay was performed according to manufacturer's instructions (Millipore Sigma). Non-infected cells were treated with NCGC2955 or analog 153 for 48-72 h, and 20 µL/well of MTT ([3-(4, 5-Dimethyl-2-thiazolyl)-2, 5-diphenyl-2 H-tetrazolium bromide], 5 mg/mL in phosphate-buffered saline (PBS) was added to each well. After shaking at 150 RPM for 5 min, the plates were incubated at 37°C for 2-3 h. Conversion of the yellow solution to dark blue formazan by mitochondrial dehydrogenases of living cells was quantified by measuring absorbance at 560 nm.

Western Blot

$2x10^6$ HFFs were plated in 6 well plates and the following day the cells were infected with OC43 (MOI-1) for one hour. Cells were then washed with PBS once and NCGC2955(1-3 µM) or emetine (1 µM) were added to infected cells. Drugs were diluted in DMEM containing 4% FBS along with non-infected and infected non-treated (DMSO only) controls. At 72 hours post infection the cells were washed with PBS and lysed in cell lysis buffer (Promega, Madison, WI) containing protease (Roche, Mannheim, Germany) and phosphatase (Thermo Fisher Scientific) inhibitors. Lysate from each condition (50 µg) was separated on 10% SDS-PAGE for detection of OC43 antigen and 25 µg lysate from each condition was analyzed for β-actin (Millipore Sigma, 1:10,000) as loading control. Anti-Coronavirus monoclonal antibody, OC-43 strain, clone 541-8F (Millipore Sigma, MAB9012) (1:250) was used to detect OC43 antigen (not defined).

Statistical analysis

Dose-response curves were generated as described (20). The EC_{50} and CC_{50} values were calculated using Graph Pad Prism software using the non-linear curve fitting and the exponential form of the median effect equation, where percent inhibition = 1/ [1+ (CC_{50} or EC_{50}/drug concentration) m], where m is a parameter that reflects the slope of the concentration-response curve.

Results

Inhibition of α-CoV with NCGC2955

Vero cells were infected with NL63 at MOI of 0.001 PFU/ cell. Immediately following infection, cells were treated with NCGC2955 (Fig. 1A, chemical structure), at concentrations ranging from 1-30 µM. NCGC2955 showed a dose response for viral RNA inhibition in the cellular compartment, EC_{50} 2.5 ± 0.15 µM (Fig. 1B). The cellular toxicity was analyzed in non-infected Vero cells at concentration of 30-300 µM. The CC_{50} was > 300 µM (Fig. 1C). In a time-course experiment, the activity of NCGC2955 was sustained and improved from 24-72 h post infection (hpi, Fig. 1D). Emetine (1 µM) reportedly inhibits α- and β-CoV *in vitro* (18), and was used as a positive control.

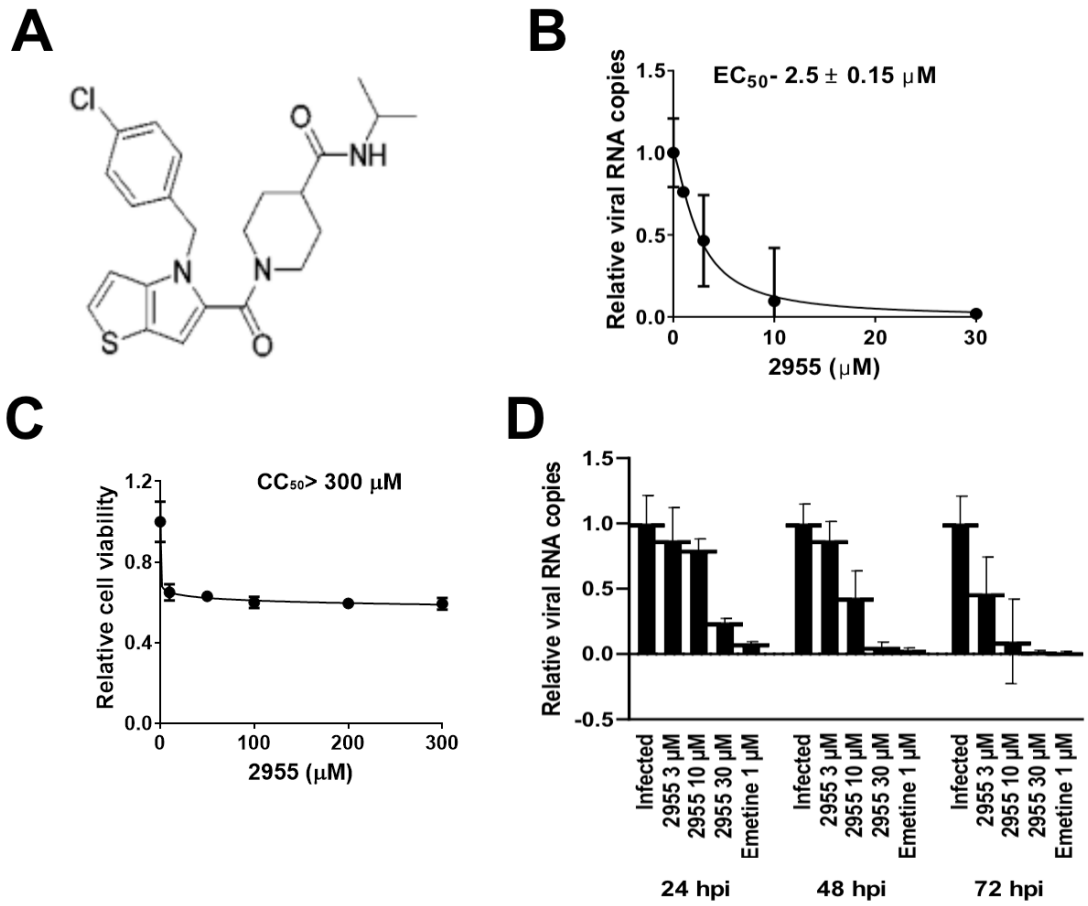

Figure 1: Anti-NL63 activity of NCGC2955 in Vero cells. **(A)** Chemical structure of NCGC2955. **(B)** Dose–response curve and EC_{50} of NCGC2955. Vero cells were infected with CoV NL63 at MOI 0.001 and treated for 72 hours with NCGC2955 ("2955") at the indicated concentrations. Viral RNA levels in cells were quantified by qRT-PCR, then normalized to the RNA level in non-treated, infected Vero cells, as well as internal normalization to cellular GAPDH RNA. The data represent mean values (± SD) of triplicate determinations from two independent experiments. **(C)** Cellular toxicity of NCGC2955 was tested by MTT assay in non-infected Vero cells at 72 h. **(D)** A time course activity of NCGC2955 was performed in infected Vero cells treated for 24, 48 and 72 h. Cell associated viral RNA levels were quantified by qRT-PCR and normalized to the RNA level in nontreated, infected Vero cells, in addition to internal normalization of each sample to cellular GAPDH RNA. Emetine (1μM) was used as positive control for anti-CoV activity. The data represent mean values (±SD) of triplicate determinations of two independent experiments.

Next, the activity of NCGC2955 was tested in NL63 infected MK2 cells. Similar to its activity in Vero cells, a dose response of NCGC2955 was observed in NL63-infected MK2 cells (EC_{50} 1.5 ± 0.2 μM, Figure 2A). The MTT curve in MK2 cells (Figure 2B) was similar to the one measured in Vero cells (Figure 1C).

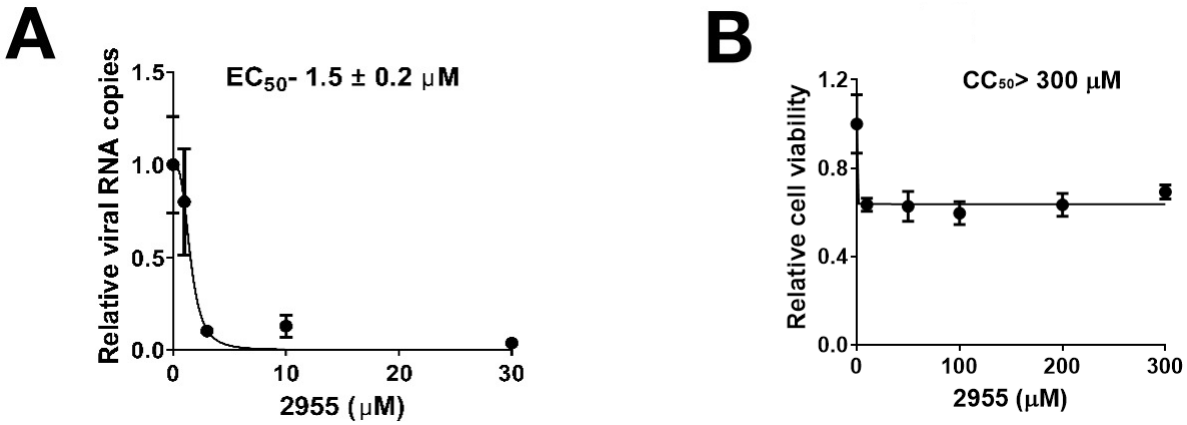

Figure 2: Anti-NL63 activity of NCGC2955 in MK2 cells. **(A)** Dose–response curve and EC_{50} value of NCGC2955. MK2 cells were infected with CoV NL63 at MOI 0.001 and treated for 72 h with NCGC2955 with the indicated compound concentrations. Viral RNA levels in cells were quantified by qRT-PCR and normalized to the RNA level in nontreated, infected Vero cells, in addition to internal normalization to cellular GAPDH RNA. **(B)** An MTT assay was performed in non-infected MK2 cells using different concentrations of NCGC2955 for 72 h. MK2 cells were also treated with DMSO (vehicle control). The data represent mean values (±SD) of triplicate determinations from two independent experiments.

Inhibition of β-CoV with NCGC2955

The activity of NCGC2955 was then measured in OC43-infected human foreskin fibroblasts (HFFs). Both viral RNA (Figure 3A) and OC43 protein (Figure 3B) were inhibited with NCGC2955.

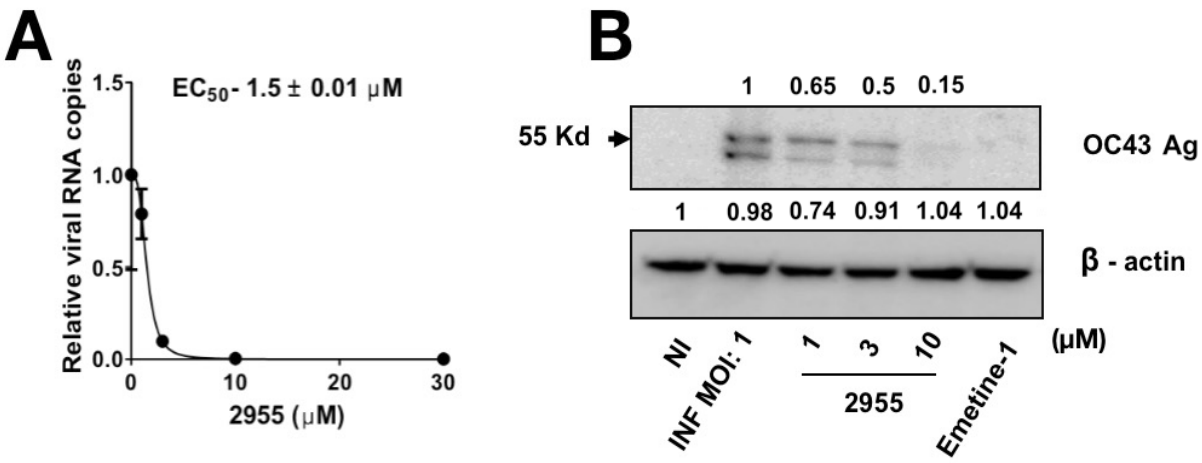

Figure 3: Anti-OC43 activity of NCGC2955 in HFF cells. **(A)** Dose–response curve and EC_{50} value of NCGC2955. HFFs were infected with OC43 at MOI 0.1 and treated for 72 h with NCGC2955 at the indicated concentrations. Cell associated viral RNA was quantified by qRT-PCR and normalized to RNA in nontreated, infected HFFs, in addition to internal normalization of each sample to cellular GAPDH RNA. The data represent mean values (±SD) of triplicate determinations from two independent experiments. **(B)** Inhibition of OC43 protein. Infected HFFs (MOI = 1) were treated for 72 h with NCGC2955 or emetine at the indicated concentration. A Western blot was performed on infected cellular lysates harvested at 72 hpi NI – noninfected control and INF – infected controls. Experiment was repeated independently twice, and data from a single representative experiment are shown.

Inhibition of SARS-CoV-2 with NCGC2955 and analog 153

Finally, the activity of NCGC2955 and analog 153 was tested against the alpha (Figure 4) and delta (Figure 5) variants of SARS-CoV2. Both compounds showed dose response inhibition of SARS-CoV-2. The 50% inhibition of the alpha variant in infected Vero E6 was 9.21 ± 0.01 μM (2955) and 6.75 ± 0.56 μM (153), based cytopathic effect (CPE), where 0 indicated complete CPE and 1 denotes 100% virus inhibition (Figure 4 A, B), and the CC_{50} of 153 in Vero E6 was > 300 μM (Figure 4C), similar to the CC_{50} of NCGC2955 (Figure 1C). In infected Calu-3 NCGC2955 and 153 showed dose response RNA inhibition (Figure 4 D, E), and CC_{50} in non-infected Calu-3 was >300 or 250 μM (Figure 4 F, G), yielding a high selectivity index of 1500 or 2500 for NCGC2955 and 153, respectively.

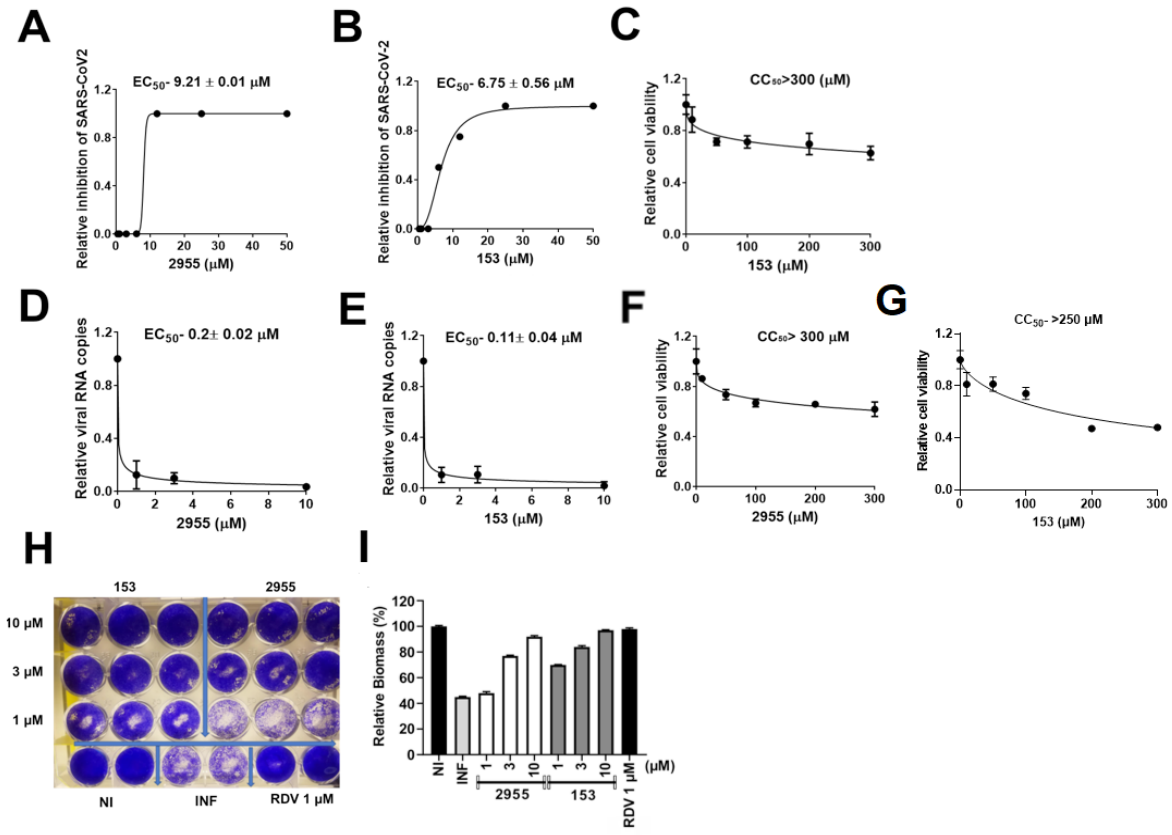

Figure 4: Inhibition of SARS-CoV-2 (alpha) by NCGC2955 and analog 153 in Vero and Calu-3 cells. (**A, B**) Dose response curves and EC_{50} values of NCGC2955 and analog 153. Vero E6 cells were infected with SARS-CoV-2 (MOI = 0.05) and treated with the indicated concentrations of drugs for 72 h. Using crystal violent, cells were then stained, and the cytopathic effect analyzed by microscopy, with a scale of 0–1 (where 0 denotes complete CPE and 1 denotes 100% virus inhibition), in each condition. The plots indicate relative inhibition compared to infected controls. (**C**) An MTT assay was performed in noninfected Vero cells using different concentrations of NCGC2955 analog 153 for 72 h. Vero cells were also treated with DMSO (vehicle control). (**D, E**) Dose response curves and EC_{50} values of NCGC2955 and analog 153. Calu-3 cells were infected with SARS-CoV2 and tested with the indicated concentrations of drugs for 48 h, supernatants were harvested, and qRT-PCR was performed. Plots on the curve specify viral RNA copies compared to infected controls. (**F, G**) An MTT assay was performed in noninfected Calu-3 cells using different concentrations of NCGC2955 and analog 153 for 48 h. Calu-3 cells were also treated with DMSO (vehicle control). (**H, I**) Biomass ODs for compounds NCGC2955 and analog 153. Calu-3 cells were infected with SARS-CoV2 and tested with the indicated concentrations of drugs for 72 h. Cells were stained with crystal violet, washed, and dissolved in 10% acetic acid, and solutions were then evaluated for absorbance at 595 nm. The plots are representative of relative biomass, where 100% biomass indicate non-infected control cells and 0% indicate complete cytopathic effect due to viral infection. Remdesivir (1μM) was used as a positive control for anti-CoV activity.

Anti-SARS-CoV-2 activity of NCGC2955 and 153 was also observed for the delta variant in Calu-3 cells, with mild increase of EC_{50} compared to inhibition of the alpha variant (Figure 5 A, B), but with overall high selectivity. Analog 153 showed better protection of the biomass at 1 µM (Figure 4 H, I), but there was no difference from NCGC2955 for the delta variant (Figure 5 C, D).

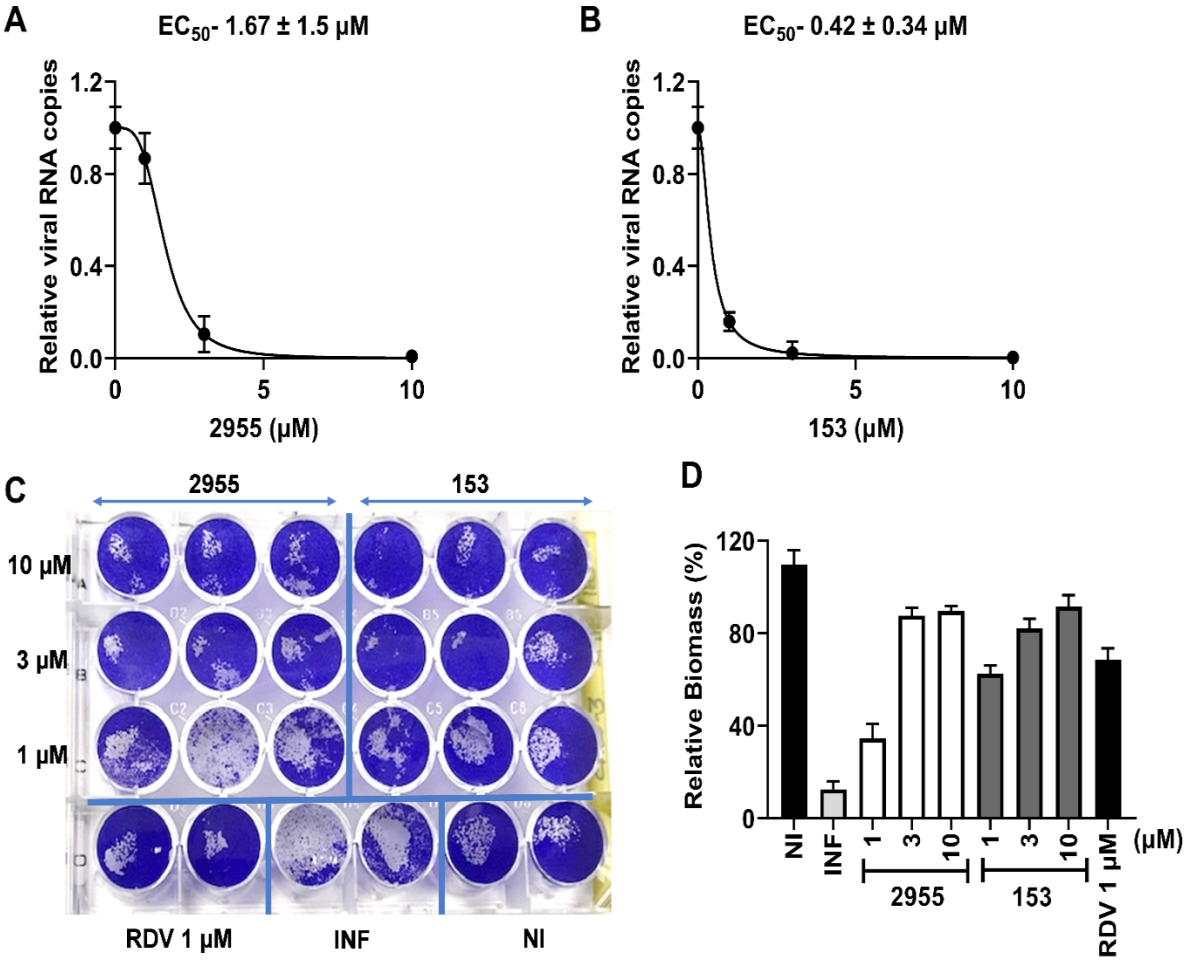

Figure 5: Inhibition of **S**ARS-CoV-2 (delta) by NCGC2955 and analog 153 in Calu-3 cells. (**A, B**) Dose response curves and EC_{50} values of NCGC2955 and analog 153. Calu-3 cells were infected with SARS-CoV2 and tested with the indicated concentrations of drugs for 72 hr. Supernatants were harvested, and qRT-PCR was performed. The plots indicate viral RNA copies compared to infected controls. (**C, D**) Biomass ODs for compounds NCGC2955 and analog 153. Calu-3 cells were infected with SARS-CoV2 and tested with the indicated concentrations of drugs for 72 h. Cells were stained with crystal violet (C), washed, dried and the stained plate was analyzed for absorbance at 595 nm. The plots are representative of relative biomass, where 100% biomass indicate non-infected control cells and 0% indicate complete cytopathic effect due to viral infection.

Discussion

A variety of drug candidates have been reported to effectively inhibit SARS-CoV-2 replication since the beginning of the pandemic. Of all studied drugs, remdesivir has been administered most commonly and showed promising clinical efficacy [3]. The protease inhibitor nirmatrelvir was studied in a phase 2–3 double-blind, randomized, controlled trial and showed reduction of progression to severe COVID-19 that was 89% lower than the risk with placebo, without evident safety concerns [21]. In late 2021 the U.S. Food and Drug Administration issued an emergency use authorization (EUA) for oral Paxlovid (nirmatrelvir/ritonavir) for the treatment of

mild-to-moderate COVID-19 in adults and children (12 years of age and older weighing at least 40 kilograms) who are at high risk for progression to severe disease. In the drug development efforts for SARS-CoV-2, all stages of virus replication are being studied, from binding to the human angiotensin-converting enzyme 2 (ACE2) [22,23], to specific SARS-CoV-2 proteins. Modulation of the host's immune response or host cell proteins/enzymes are also under consideration. Drugs that specifically target viral proteins are likely to have higher selectivity against the virus, but drug resistance may develop, particularly in RNA viruses where mutations occur frequently. Targeting host cells may prevent and slow the development of drug resistance, but the concern remains for the doses that are needed for virus suppression and the potential for adverse effects [24].

The rationale for testing the anti-CoV activity of NCGC2955 was based on recent findings from our laboratory that it inhibits human cytomegalovirus replication, and previous reports of structurally related compounds that inhibit RNA viruses [14,15]. It was our hypothesis that the pan anti-viral activity observed in piperidine-4-carboxamide analogs NCGC2955 and CCG205432 might extend to anti-CoV activity. Piperidine-4-carboxamide analogs were studied in detail in cell-based assays using Western Equine Encephalitis virus (WEEV) replicons and showed half-maximal inhibitory concentrations of ~ 1 μM and selectivity indices of >100. CCG205432, similar to our 153 analog (the TFA salt of CCG205432) inhibited infectious virus in cultured human neuronal cells. These compounds show broad inhibitory activity against RNA viruses in culture, including members of the *Togaviridae*, *Bunyaviridae*, *Picornaviridae*, and *Paramyxoviridae* families. Their mechanism-of-action may involve a host factor that modulates cap-dependent translation. CCG205432 did not directly target WEEV RNA dependent RNA polymerase or other viral enzyme activities that would promote the development of drug-resistant viral mutants. More recently, piperidine-4-carboxamides were reported to inhibit *Mycobacterium abscessus* DNA gyrase [25]. *N*-aryl-piperidine-4-carboxamides were reported to inhibit MALT1 proteolytic activity which is critical in activation of the NF-κB pathway [26], and 4-piperidone conjugates were described possessing antiviral properties against SARS-CoV-2 [27,28].

Our studies reveal that NL63, OC43 and SARS-CoV-2 variants alpha and delta are inhibited by NCGC2955 and 153 at low μM concentration. The selectivity index of both compounds (CC_{50}/ EC_{50}) was favorable, based on CC_{50} of > 300 μM in all tested cell lines. NCGC2955 and 153 analog inhibited SARS-CoV-2 in both Vero E6 and Calu-3 cells at sub-μM concentrations. The biomass preservation in alpha infected Calu-3, and the EC_{50} of the RNA in delta-infected Calu-3 cells suggest improved activity of 153 compared to NCGC2955.

The activity of both analogs against SARS-CoV-2 infected Vero E6 cells was reduced compared to SARS-CoV-2 inhibition in Calu-3 cells. Differences observed in virus inhibition could be cell-based and/or reflect virus susceptibility [29,30]. Remdesivir, first tested by RT-PCR in Vero E6, was shown to be active against SARS-CoV-2, with an EC_{50} of ~0.77 μM. It was shown that the 50% cytopathic effect was much higher than the RNA suppression, when comparing its antiviral activity on clinical isolates of SARS-CoV-2 in Vero E6 cells. The Hong Kong/VM20001061/2020 strain also showed lower susceptibilities of SARS-CoV-2 clinical isolates to remdesivir [31], suggesting that a combination therapy of remdesivir with emetine can be used, based on *in vitro* synergy.

Although we expect to see a correlation of *in vitro* activity of a compound with *in vivo* activity this is not easily achieved due to pharmacokinetic and pharmacodynamic parameters. In addition, agents with broad activity against viruses/microorganisms may act through host-derived mechanisms that are cell-specific. Therefore, for future studies that repurpose drugs for infectious disease, identification of these mechanisms is critical. Though *in vivo* drug concentrations are measured in blood, we must also consider concentrations at the site of infection. The drug concentrations achieved in the lung parenchyma in respiratory tract infections, for instance, may determine the efficacy of that given drug. Oseltamivir, as an example, has high bioavailability and penetrates infection sites at concentrations sufficient enough to inhibit influenza replication [32]. Since indole analogs have shown improved outcomes (both symptoms and survival) in an *in vivo* mouse model of alphaviral encephalitis, and a mouse PK study demonstrated that chemical modifications can improve plasma drug exposures, it is possible that NCGC2955 and analog 153 may also have *in vivo* activity against SARS-CoV2, although their PK profile has not been established for this indication [14,15]. In our human cytomegalovirus investigation we observed that the indole can be replaced with other similarly substituted heterocycles without significant impact on potency [17]. Thus, the indole may not be making critical interactions with the target but may serve to hold the molecule in a preferred geometry. Further investigation of related compounds against SAR-CoV2 is warranted. These studies may pave the way towards the development of safe broad-spectrum antiviral agents.

Conclusion

Analogs of piperidine-4-carboxamides inhibit coronaviruses including SARS-CoV-2 at low μM concentrations and can be further developed as broad-spectrum antiviral agents.

Acknowledgments

Supported by the Flight Attendant Medical Research Institute (FAMRI) and the Institute for Clinical and Translational Research

(UL1TR003098), DJM, and the Department of Pediatrics, Medical College of Wisconsin (RAB).

References

1. Zhou P, Yang XL, Wang XG, Hu B, Zhang L, et al., (2020) A pneumonia outbreak associated with a new coronavirus of probable bat origin. Nature 579:270-273.
2. Dhama K, Sharun K, Tiwari R, Dadar M, Malik YS, et al., (2020) COVID-19, an emerging coronavirus infection: advances and prospects in designing and developing vaccines, immunotherapeutics, and therapeutics. Hum Vaccin Immunother 16:1232-1238.
3. Beigel JH, Tomashek KM, Dodd LE, Mehta AK, Zingman BS, et al., (2020) Remdesivir for the Treatment of Covid-19 - Final Report. N Engl J Med 383:1813-1826.
4. Shyr ZA, Gorshkov K, Chen CZ, Zheng W (2020) Drug Discovery Strategies for SARS-CoV-2. J Pharmacol Exp Ther 375:127-138.
5. Bernal JA, Gomes da Silva MM, Musungaie DB, Kovalchuk E, Gonzalez A, et al., (2022) Molnupiravir for Oral Treatment of Covid-19 in Nonhospitalized Patients. N Engl J Med 386:509-520.
6. Mahase E (2021) Covid-19: Pfizer's paxlovid is 89% effective in patients at risk of serious illness, company reports. BMJ 375:n2713.
7. Pyrc K, Berkhout B, van der Hoek L (2007) Identification of new human coronaviruses. Expert Rev Anti Infect Ther 5:245-253.
8. Chu CM, Cheng VCC, Hung IFN, Wong MML, Chan KH, et al., (2004) Role of lopinavir/ritonavir in the treatment of SARS: initial virological and clinical findings. Thorax 59:252-256.
9. Cao B, Wang Y, Wen D, Liu W, Wang J, et al., (2020) A Trial of Lopinavir-Ritonavir in Adults Hospitalized with Severe Covid-19. N Engl J Med 382:1787-1799.
10. Ferner RE, Aronson JK (2020) Chloroquine and hydroxychloroquine in covid-19. BMJ 369:m1432.
11. Ferner RE, Aronson JK (2020) Remdesivir in covid-19. BMJ 369:m1610.
12. Luo P, Liu Y, Qiu L, Liu X, Liu D, et al., (2020) Tocilizumab treatment in COVID-19: A single center experience. J Med Virol 92:814-818.
13. Chen P, Nirula A, Heller B, Gottlieb RL, Boscia J, et al., (2021) SARS-CoV-2 Neutralizing Antibody LY-CoV555 in Outpatients with Covid-19. N Engl J Med 384:229-237.
14. Delekta PC, Dobry CJ, Sindac JA, Barraza SJ, Blakely PK, et al., (2014) Novel indole-2-carboxamide compounds are potent broad-spectrum antivirals active against western equine encephalitis virus in vivo. J Virol 88:11199-214.
15. Sindac JA, Barraza SJ, Dobry CJ, Xiang J, Blakely PK, et al., (2013) Optimization of novel indole-2-carboxamide inhibitors of neurotropic alphavirus replication. J Med Chem 56:9222-41.
16. Kapoor A, Ghosh AK, Forman M, Hu X, Ye W, et al., (2020) Validation and Characterization of Five Distinct Novel Inhibitors of Human Cytomegalovirus. J Med Chem 63:3896-3907.
17. Guo, X, Ghosh AK, Keyes RF, Peterson F, Forman M, et al., (2022) The Synthesis and Anti-Cytomegalovirus Activity of Piperidine-4-Carboxamides. Viruses 14:234.
18. Shen, L, Niu J, Wang C, Huang B, Wang W, et al., (2019) High-Throughput Screening and Identification of Potent Broad-Spectrum Inhibitors of Coronaviruses. J Virol 93:e00023-19.
19. Fan YH, Roy S, Mukhopadhyay R, Kapoor A, Duggal P, et al., (2016) Role of nucleotide-binding oligomerization domain 1 (NOD1) and its variants in human cytomegalovirus control in vitro and in vivo. Proc Natl Acad Sci U S A 113:E7818-E7827.
20. Cai H, Kapoor A, He R, Venkatadri R, Forman M, et al., (2014) In vitro combination of anti-cytomegalovirus compounds acting through different targets: role of the slope parameter and insights into mechanisms of Action. Antimicrob Agents Chemother 58:986-994.
21. Hammond J, Leister-Tebbe H, Gardner A, Abreu P, Bao W, et al., (2022) Oral Nirmatrelvir for High-Risk, Nonhospitalized Adults with Covid-19. N Engl J Med 386:1397-1408.
22. Monteil V, Kwon H, Prado P, Hagelkrüys A, Wimmer RA, et al., (2020) Inhibition of SARS-CoV-2 Infections in Engineered Human Tissues Using Clinical-Grade Soluble Human ACE2. Cell 181:905-913 e7.
23. Song LG, Xie QX, Lao HL, L ZY (2021) Human coronaviruses and therapeutic drug discovery. Infect Dis Poverty 10:28.
24. Hoenen T, Groseth A, Feldmann H (2019) Therapeutic strategies to target the Ebola virus life cycle. Nat Rev Microbiol 17:593-606.
25. Negatu DA, Beuchel A, Madani A, Alvarez N, Chen C, et al., (2021) Piperidine-4-Carboxamides Target DNA Gyrase in Mycobacterium abscessus. Antimicrob Agents Chemother 65:e0067621.
26. Schlapbach A, Revesz L, Soldermann CP, Zoller T, Régnier CH, et al., (2018) N-aryl-piperidine-4-carboxamides as a novel class of potent inhibitors of MALT1 proteolytic activity. Bioorg Med Chem Lett 28:2153-2158.
27. Srour AM, Panda SS, Mostafa A, Fayad W, El-Manawaty MA, et al., (2021) Synthesis of aspirin-curcumin mimic conjugates of potential antitumor and anti-SARS-CoV-2 properties. Bioorg Chem 117:105466.
28. Youssef MA, Panda SS, Aboshouk DR, Said MF, Taweel AE, et al., (2022) Novel Curcumin Mimics: Design, Synthesis, Biological Properties and Computational Studies of Piperidone-Piperazine Conjugates. ChemistrySelect 7:e202201406.
29. Malin JJ, Suárez I, Priesner V, Fätkenheuer G, Rybniker J (2020) Remdesivir against COVID-19 and Other Viral Diseases. Clin Microbiol Rev 34:e00162-20.
30. Ghosh AK, Miller H, Knox K, Kundu M, Henrickson KJ, et al., (2021) Inhibition of Human Coronaviruses by Antimalarial Peroxides. ACS Infect Dis 7:1985-1995.
31. Choy KT, Wong AYL, Kaewpreedee P, Sia SF, Chen D, et al., (2020) Remdesivir, lopinavir, emetine, and homoharringtonine inhibit SARS-CoV-2 replication in vitro. Antiviral Res 178:104786.
32. Davies BE (2010) Pharmacokinetics of oseltamivir: an oral antiviral for the treatment and prophylaxis of influenza in diverse populations. J Antimicrob Chemother 65:ii5-ii10.